

SYNTHESIS AND CHARACTERIZATION OF UNIFORM PRASEODYMIUM DOPED ANATASE TiO₂ NANOPARTICLES

Mariñoso Pascual, Juan Manuel; Gómez Lopera, Salvador Ángel
Universidad Politécnica de Cartagena

In this work a new synthesis method of uniform praseodymium doped anatase TiO₂ nanoparticles and pseudoellipsoidal shape is described. The resultant nanoparticles are good candidates to be employed in catalysis, energy storage and photovoltaic energy production applications. The synthesis is a gel-sol process using a shape controlled by seeding of anatase TiO₂:Pr. Three doped systems at 1%, 5%, 10% [Pr]/[Ti] molar mass ratio were prepared. Pure anatase system with and without seeds was also synthesized to compare with doped systems. XRD and EDX analysis showed praseodymium inserted in anatase bulk structure for lower doped values, formless structure at the highest doped value, and real doping ratio 2%, 3% and 9% respectively. TEM pictures confirm monodisperse nanoparticles with pseudoellipsoidal shape. The average diameter of the semi-major axis is 14.1±0.6 nm and 16.2±0.7 nm for pure anatase with and without seeds, and 14.0±0.8 nm for the 3% doped system. In order to assess crystalline structure parameters a Rietveld refinement with FULLPROF software was done. Results for 3% doped system shows an interplanar distance of 0.35 nm (this was checked by direct measurements on TEM pictures), an increase in cell volume and similar crystallite size (around 12 nm) respect undoped systems.

Keywords: Nanoparticles; Doping; Monodisperse; Anatase; Refinement; Gel-sol

SÍNTESIS Y CARACTERIZACIÓN DE NANOPARTÍCULAS PSEUDOELIPSOIDALES UNIFORMES DE TiO₂ ANATASA DOPADA CON PRASEODIMIO

Presentamos un nuevo método de síntesis de nanopartículas uniformes de TiO₂ anatasa dopadas con praseodimio y forma pseudoelipsoidal. Las partículas resultantes son buenos candidatos para aplicaciones de catálisis, almacenamiento de energía y producción de energía fotovoltaica. La síntesis es un proceso gel-sol que utiliza semillas de anatasa dopada TiO₂:Pr para controlar la forma. Se preparó tres sistemas dopados de razón molar [Pr]/[Ti] 1%, 5%, 10% y anatasa pura -con y sin semillas. Los análisis DRX y EDX demuestran que el praseodimio está incluido en la estructura de la anatasa para valores bajos de dopado, estructura amorfa para el mayor dopado y porcentajes reales de dopado de 2%, 3% y 9% respectivamente. Las imágenes MET confirman nanopartículas monodispersas y pseudo-elipsoidales. El diámetro medio del semieje mayor es de 14.1±0.6 nm y 16.2±0.7 nm para anatasa pura con y sin semillas, y 14.0±0.8 nm para el 3%. Se ha realizado un refinamiento Rietveld con el software FULLPROF para obtener los parámetros cristalinos, destacando para el sistema al 3% una distancia interplanar de 0.35 nm (hecho verificado sobre imágenes MET), un incremento del volumen de la celda y un tamaño similar (unos 12 nm) con respecto a anatasa pura.

Palabras clave: Nanopartículas; Dopado; Monodispersión; Anatasa; Refinamiento; Gel-Sol

Correspondencia: Salvador Ángel Gómez Lopera - salvador.glopera@upct.es

Agradecimientos: Los autores agradecemos al Departamento de Física Aplicada y al grupo de I+D "Nanopartículas y Dispersiones" de la UPCT la financiación de este trabajo

1. Introduction

Many reports are dedicated about TiO_2 due to good properties and wide industrial applications, such as catalysis, storage, environmental clean-up and solar cells. It is very common to find doped TiO_2 , because its width band gap is about 3.2 eV, enough high to semiconductor use, and it is interesting to replace atoms in bulk structure to narrow band gap (Renhui *et al.*, 2012). Among others researchers usually want to select a way to tailor a material with high crystallinity, morphology adjustable, specific phases, optical properties (Zhang *et al.*, 2012) and effects by structural order-disorder (Silva Junior *et al.*, 2015). For structural studies there are some software of Refinement based in Rietveld like TOPAS (Rangel-Vázquez *et al.*, 2015), GSAS (Silva Junior *et al.*, 2015) or FULLPROF (Ma *et al.*, 2014), (Delekar *et al.*, 2012), the last one was selected to use in our theoretical characterization. Other possibilities in doped titania, referee in rare earth to get unique luminescence properties because $4f$ transitions, just studied from experimental study (Leostean *et al.*, 2013), (Ricci *et al.*, 2013), or using Density Functional Theory (Liang *et al.*, 2009), (Khan *et al.*, 2012), even in Silica aerogel (Amlouk *et al.*, 2008). There are many synthesis methods along literature to get nanostructures (Wang *et al.*, 2014), and more specify nanoparticles, among them, it is usual to find hydrolysis, hydrothermal and sol-gel methods under variations. Sol-gel is well-known to control doping and nanoparticle size. However, if uniform nanoparticles are required will not to be easy controlling of size at the same time. Sugimoto's technic (2007) in gel-sol method allow to get uniform and controlled size nanoparticles. In this work, we have modified the Sugimoto's technic, in order to obtain praseodymium doped uniform nanoparticles.

2. Experimental

2.1. Synthesis

The nanoparticles under seeding process was getting as the complex route of Sugimoto, Zhou and Muramatsu (2003), thus it was made a colloid suspension of nanoparticles seeds before. The dopant step was introduce at first of sequence for manufacture of both seeds and nanoparticles, when the first precipitate of hydroxide gel is forming. Four kinds of seeds were made at 0% (pure anatase), 1%, 5% and 10% [Pr]/[Ti] molar mass ratio, four kind of nanoparticles from seeds previously synthesized and a pure anatase system without seeds. All reagents used were purchased from Sigma-Aldrich. First seed particles of anatase TiO_2 were prepared to produce the growth of main nanoparticles anatase using as precursor titanium (IV) isopropoxide (TIPO) and stabilizer triethanolamine (TEOA) at 99.999% and 99% in purity percentage respectively. After [Pr]/[Ti] molar mass ratio was selected, it was dropped pure liquid TIPO in Milli-Q water with Cl_3Pr to get 0.25 mol dm^{-3} of Ti^{+4} in stock solution. Then solution was adjusted down to pH 1.3 with HClO_4 , and the system aged at 100°C in order to obtain seeds. Afterward taking a molar seeds ratio [seeds]/[TIPO] at 0.025 of seed suspension was dispersed by ultrasonification for 30 min. While molar ratio TIPO:TEOA = 1.1:1.0 were prepared with the middle of final stock solution with the same Ti^{+4} molar ratio and Cl_3Pr with the same [Pr]/[Ti] using before, which were undergone to magnetic stirring for 30 min. Then it was added enough TEOA to achieve a molar ratio TIPO:TEOA = 1:2 using the mixture of pure liquids in the same fixed volume of the solution and Ti^{+4} concentration of experiment above and was adjusted to get round pH 9 value. Finally 25 cm^3 of compound solution Ti^{+4} stable against hydrolysis was aged at 100°C for 24 h for gelation and for its nucleation of the highly viscous gel was exposed under second aging at 140°C for 72 h. In manufacturing pure nanoparticles of anatase without seeds it was prepared a molar ratio TIPO:TEOA = 1:2 in 0.25 mol dm^{-3} of Ti^{+4} using the same solution volume of experiments before. Final solution was adjusted round pH 9 value and aged at 100°C for 24 h for gelation and 140°C for 72 h to nucleate and grow nanoparticles.

2.2. X-Ray Powder Diffraction

Experiments of X-Ray Powder Diffraction (XRD) were performed to obtain samples crystallinity, specify structure, lattice parameters, average crystallite sizes and average maximum micro strain. Spectral diffractions were recorded at room temperature by a Bruker D8 Advance Instrument, equipped by first Soller, 1 mm divergence slit and undispersed display, second 2.5° Soller, 8 mm receiving slit and a Nickel filter. Samples were exposed under CuK α beams radiation at 40 kV x 3 mA. The experiments carried out from 10° to 70° in 2 θ space with step size 0.02° wide, using one second for step time. A powder Corundum sample was used to achieve a standard instrument resolution function. Each XRD pattern was analyzed with Rietveld method using FULLPROF suite package, by Rodriguez-Carvajal (2001). Selected background mode was a linear interpolation between a set of points clever chosen. Thompson-Cox-Hastings pseudo-Voigt with axial divergence asymmetry (TCH) like Peak shape was used to fit with mimic convolution of Lorentzian and Gaussian function. Summarized refinement parameters are arranged in Table 1. In the refinement process were allowed to vary scale factor, background points, cell parameters, FWHM parameters, shape parameters, atoms position, thermal factors, preferred orientation coefficient and occupancy factor under Profile Matching Mode. Whole of data calculated were done with only one phase I41/amd. Tries to get another possible hidden phase were unsuccessful.

Table 1. Summary of structural data refinement

Parameters	Pr/Ti mass expected ratio (%)			
	0(*)	0	1	5
Space group	I41/amd			
a (Å)	3.7942 (1)	3.7959 (1)	3.7940 (1)	3.7960 (9)
c (Å)	9.5032 (2)	9.4985 (3)	9.4951 (3)	9.4892 (22)
V (Å) ³	136.804 (5)	136.861 (7)	136.680 (7)	136.74 (6)
Ti (4a)	(0, 3/4, 1/8)	(0, 3/4, 1/8)	(0, 3/4, 1/8)	(0, 3/4, 1/8)
O (8e)	(0,1/4,0.08588 (1))	(0,1/4,0.08646 (1))	(0,1/4, 0.0854 (3))	(0,1/4, 0.0871 (3))
Pr (4a)	-	-	(0, 3/4, 1/8)	(0, 3/4, 1/8)
R _p , R _{wp} , R _e , χ^2	7.75,7.23,6.34,1.30	8.07,7.59,6.66,1.30	11.0,9.68,8.32,1.35	10.2, 9.64, 7.12, 1.83
Crystallite size (Å)	151.36 (0)	124.66 (4)	137.01 (0)	88.57 (0)
Max. strain (%%)	9.088 (3)	20.228 (8)	24.41 (1)	6.929 (2)

(*) Sample without seeds

2.3. Transmission and Scanning Electron Microscope

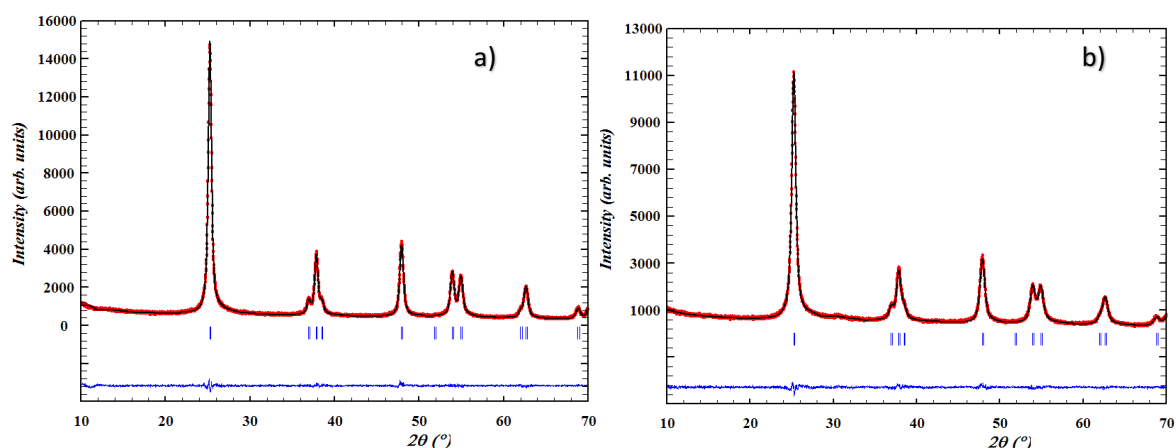
TEM measurements were achieved by JEOL JEM-2100 instrument (200 kV maximum acceleration potential, LaB₆ filament) and X-ray energy dispersive spectrometer (EDS) equipment (K α peak resolution of Mn at 133 eV mm⁻²). Others EDS measurements were carried out in SEM equipment (K α peak resolution of Mn in middle high at 128 eV). Samples were prepared in a dispersed particles immersion using Milli-Q water on carbon coated copper grid and dried in oven at 60 °C between 2-3 hours.

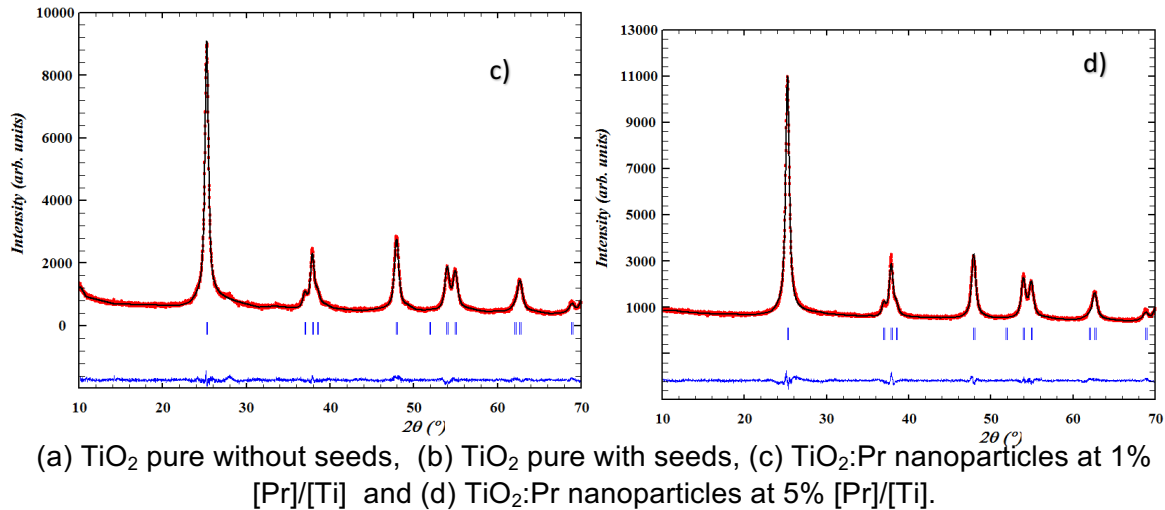
3. Results and discussion

Different samples were produced to understand the changes carried out by seeding and doped procedure. EDS measurements for doped samples show the presence of Pr species and a good agreement by seeking percentage, with 2%, 3% and 9% for 1%, 5% and 10% weight percent originally selected.

X-ray results shows maximum high crystallinity in undoped and without seeds, and a decreasing intensity from undoped sample to maximum doped sample as it is shown in Figure 1. Proposed phase agree on structural parameters referee with anatase phase. In seeking about other kind of phase, trying different space group sharing with I41/amd like P321 in Pr₂O₃ was carried out, but using DIFRACC.EVA v.3.0 program by Brucker AXS to evaluate a previously study at different percentages values was not found this possible underhand phase, in this way we discriminated possibility to include it or not in refinements studies. For before conclusion the reasoning of doped insert like doped interstitial was undergone. This kind of possibility depend on bonds built, and there is only one simple oxide with Pr specie linked with close oxygens neighbors. All experiments were carried out using an instrument function with very high crystallinity to correct the instrument broadening influence. It was selected a TCH profile function to refine, this way is easier adjust theoretical points using a specific width mixed Gaussian and Lorentzian influence function. Possible Axial divergence by bad instrumental calibration is corrected with the same function, trying to mimic the sensitive impact. FULLPROF give an integral breadth method to obtain averages of sizes and strains, from only phenomenological treatment due to structural defects.

Figure 1: Refinement by Rietveld method. XRD patterns





All goodness of fit parameters take suitable values, with χ^2 between 2 and 1. Lattice parameters change at the same step than crystallite size, while a lattice parameter is oscillating, *c* is decreasing with increase of Pr concentration.

It is noted an increase of crystallinity when this system is compared with seeds against system without those. This is clear seeing decrease of size in pure system with seeds regarding pure system without seeds as reported in table 1, high crystalline is reported in other works (*Spadavecchia et al., 2012*). On the other hand, there is a jump behavior in doped system at 1% [Pr]/[Ti] sample increasing crystallinity respect pure anatase with seeds. In other samples, crystallinity decreasing with the insert Pr species in the bulk cause of decreasing crystallite size such as it expected.

Main anatase planes (101) are identified in crystallites pictures from TEM observations (Figure 2) what corroborates high crystallinity and the same value from refinement about 0.35 nm.

From measure of polydispersity (Hunter, 2001), we asses that samples are monodispersed. Polydispersity and coefficient of variation formula is given by

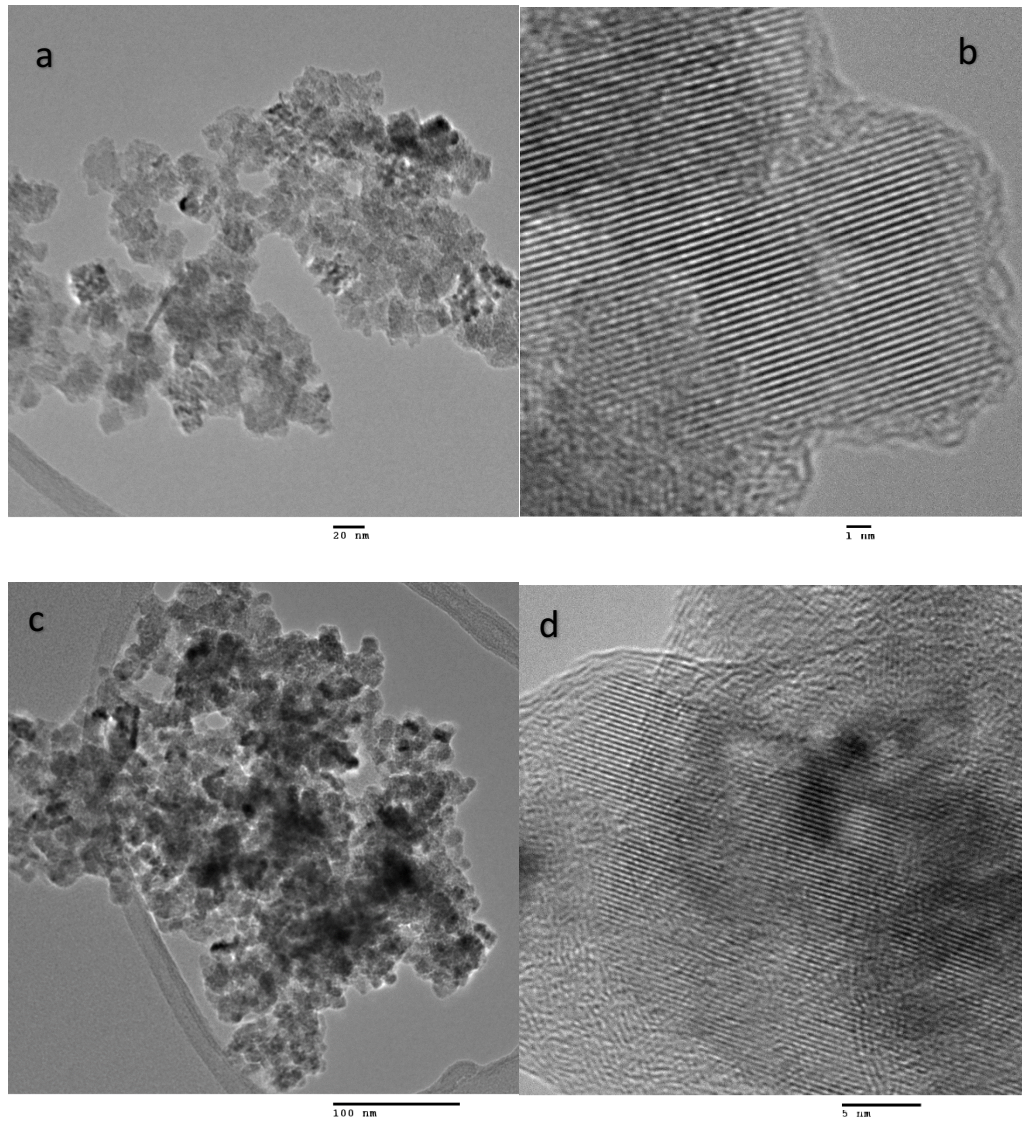
$$P_d = \left[1 + \frac{\sigma^2}{\bar{d}} \right]^{1/2} \quad (1)$$

$$C = \frac{\sigma}{\bar{d}} \times 100\% \quad (2)$$

where P_d is Polydispersity, C is the coefficients of variation, σ typical deviation and \bar{d} mean of the diameters.

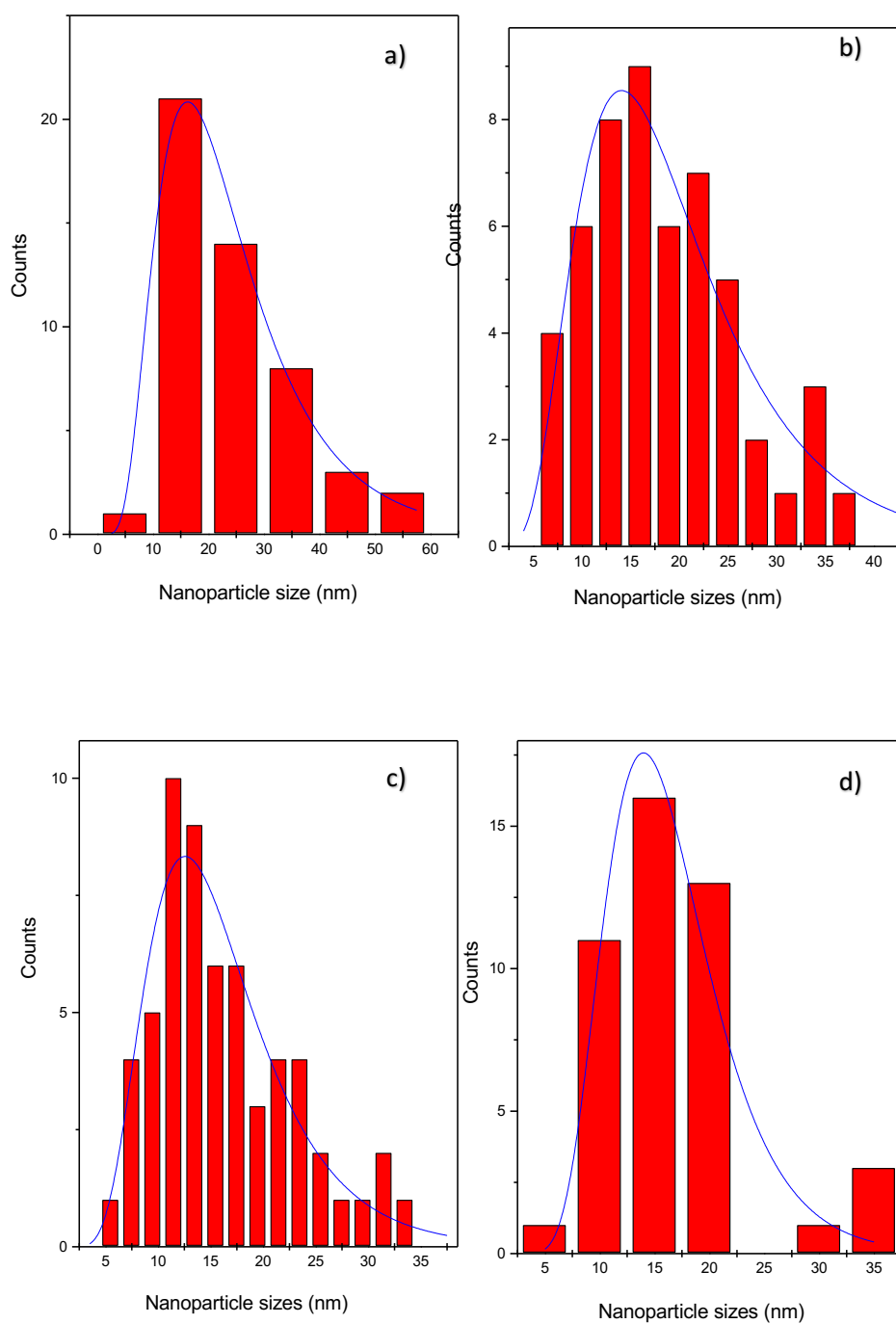
Polydispersity values are 1.0009, 1.0020 and 1.0019 and the coefficients of variation are 4.3%, 6.3% and 6.2% respectively for TiO₂ pure anatase with seeds, without seeds and doped anatase for EDX measured 3% weight percent. Nanoparticles average diameter of the semi-major axis were also studied from TEM pictures. A normal logarithmic function fit of graphs of Figure 3 provides 14.1 ± 0.6 nm and 16.2 ± 0.7 nm for pure anatase with and without seeds, and 12.6 ± 0.4 nm and 14.0 ± 0.8 nm for 2% and 3% weight percent respectively.

Figure 2: TEM pictures of $\text{TiO}_2\text{:Pr}$ nanoparticles



(a) $\text{TiO}_2\text{:Pr}$ nanoparticles at 1% [Pr]/[Ti]. (b) Crystallite anatase plane (101) for 1% [Pr]/[Ti].
(c) $\text{TiO}_2\text{:Pr}$ nanoparticles at 5% [Pr]/[Ti]. (d) Crystallite anatase plane (101) for 5% [Pr]/[Ti].

Figure 3: Histograms of semi-major axis of nanoparticles and normal logarithm fits



(a) TiO_2 pure without seeds. (b) TiO_2 pure with seeds. (c) $\text{TiO}_2\text{:Pr}$ nanoparticles at 1% $[\text{Pr}]/[\text{Ti}]$. (d) $\text{TiO}_2\text{:Pr}$ nanoparticles at 5% $[\text{Pr}]/[\text{Ti}]$.

4. Conclusions

Uniform praseodymium doped anatase ($\text{TiO}_2\text{:Pr}$) nanoparticles with different $[\text{Pr}]/[\text{Ti}]$ molar mass ratios have been successfully achieved by a new method of synthesis. EDX confirms Pr specie was found in doped samples at percent very close to selected initially. XRD shows Pr dopant embedded into the bulk anatase structure and causes a growth of volume as confirmed by refinement studies. Dopant structures reduces their crystallinity respect to pure anatase with seeds, and so much respect pure anatase without seeds, so we can conclude seeds in preparation samples reduces crystallinity as well as crystallite sizes. Lattice parameters shows a several reduction in c with doping increasing and a variation in a , increasing in anatase pure without seeds respect to pure with seeds, decreasing at 2% dopant and increasing at 3%. We conclude Pr species narrow unit cell lightly in a -axis and acutely in c -axis, and seeds influences more in pure anatase.

5. References

- Amlouk, A., El Mir, L., Kraiem, S., Saadoun, M., Alaya, S., & Pierre, A.C. (2008). Luminescence of $\text{TiO}_2\text{:Pr}$ nanoparticles incorporated in silica aerogel. *Materials Science and Engineering B*, 146, 74-79.
- Brucker AXS, "DIFRACC.EVA v.3.0". Copyright 2013.
- Delekar, S.D., Yadav, H.M., Achary, S. N., Meena, S. S., & Pawar, S.H. (2012). Structural refinement and photocatalytic activity of Fe-doped anatase TiO_2 nanoparticles. *Applied Surface Science*, 263, 536-545.
- Hunter, R.J. (2001). *Foundations of Colloid Science* (2). New York: Oxford University Press.
- Khan, M., Xu, J., Chen, N., & Cao, W. (2012). Electronic and optical properties of pure and Mo doped anatase TiO_2 using GGA and GGA+U calculations. *Physica B*, 407, 3610-3616.
- Leostean, C., Stefan, M., Pana, O., Cadis, A.L., Suciu, R.C., Silipas, T.D., & Gautron, E. (2013). Properties of Eu doped TiO_2 nanoparticles prepared by using organic additives. *Journal of Alloys and Compounds*, 575, 29-39.
- Liang, B., Mianxin, S., Tianliang, Z., Xiaoyong Z., & Qingqing, D. (2009). Band gap calculation and photo catalytic activity of rare doped rutile TiO_2 . *Journal of rare earths*, 27, 461.
- Ma, Z., Wang, Y., Sun, C., Alonso, J. A., Fernández-Díaz, M. T., & Chen, L. (2014). Experimental visualization of the diffusion pathway of sodium ions in the $\text{Na}_3[\text{Ti}_2\text{P}_2\text{O}_{10}\text{F}]$ anode for sodium-ion battery. *Scientific Reports*, 4, 7231.
- Rangel-Vázquez, I., Del Angel, G., Bertin, V., González, F., Vázquez-Zavala, A., Arrieta, A., Padilla, J.M., Barrera, A., & Ramos-Ramirez, E. (2015). Synthesis and characterization of Sn doped TiO_2 photocatalysts: Effect of Sn concentration on the textural properties and on the photocatalytic degradation of 2,4-dichlorophenoxyacetic acid. *Journal of Alloy and Compounds*, 643, S144-S149.
- Ricci, P.C., Carbonaro, C.M., Geddo Lehmann, A., Congiu, F., Puxeddu, B., Cappelletti, G., & Spadavecchia, F. (2013). Structure and photoluminescence of TiO_2 nanocrystals doped and co-doped with N and rare earths (Y^{+3} , Pr^{+3}). *Journal of Alloys and Compounds*, 561, 109-111.
- Rodriguez-Carvajal, J. (2001). Recent developments of the program FULLPROF. *Commission on powder diffraction (IUCr)*. Newsletter, 26, 12-19.

- Silva Junior, E., La Porta, F. A., Liu, M. S., Andrés, J., Varela, J. A., & Longo, E. (2015). A relationship between structural and electronic order–disorder effects and optical properties in crystalline TiO₂ nanomaterials. *Dalton Transactions*, 44, 3159-3175.
- Spadavecchia, F., Cappelletti, G., Ardizzone, S., Ceotto, M., Simone Azzola, M., Lo Presti., L., Cerrato, G., & Falciola, L. (2012). Role of Pr on the Semiconductor Properties of Nanotitania. An Experimental and First-Principles Investigation. *The Journal of Physical Chemistry C*, 116, 23083-23093.
- Sugimoto, T. (2007). Underling Mechanisms in size control of uniform nanoparticles. *Journal of Colloid and Interface Science*, 309, 106-118.
- Sugimoto, T., Zhou, X., & Muramatsu, A. (2003). Synthesis of uniform anatase TiO₂ nanoparticles by gel-sol method 3. Formation process and size control. *Journal of Colloid and Interface Science*, 259, 43-52.
- Wang, Y., He, Y., Lai, Q., & Fan, M. (2014). Review of the progress in preparing nano TiO₂: An important environmental engineering material. *Journal of Environmental Science*, 26, 2139-2177.
- Zhang, R., Wang, Q., Liang, J., Li, Q., Dai, J., & Li, W. (2012). Optical properties of N and transition metal R (R=V, Cr, Mn, Fe, Co, Ni, Cu and Zn) codoped anatase TiO₂. *Physica B*, 407, 2709-2715.